Restoring WC in plasma sprayed WC–Co coatings through spark plasma sintering (SPS)

L.G. Yu[a], K.A. Khor[a,*], H. Li[a], K.C. Pay[b], T.H. Yip[b], P. Cheang[b]

[a]School of Mechanical and Production Engineering, Nanyang Technological University, 50 Nanyang Avenue, Singapore 639798, Singapore
[b]School of Materials Engineering, Advanced Materials Research Centre (AMRC), Nanyang Technological University, 50 Nanyang Avenue, Singapore 639798, Singapore

Abstract

Decarburization of WC–Co is a common phenomenon during atmospheric plasma spray (APS) deposition, resulting in a large amount of W_2C and other carbon-deficient phases in the coating. Consequently, the properties and performance of the coating may be inadequate and unreliable. In this study, spark plasma sintering (SPS) is applied as a post-spray heat treatment to reinstate the WC phase in the APS WC/Co coating. Three sets of sample configurations have been employed, namely: direct contact of graphite punch with APS WC–Co coating, packing the coating in WC–Co powder, and finally, packing APS WC–Co coatings in yttria-stabilized zirconia (YSZ) powder. The treatment was carried out at 800 °C for 5 min. Scanning electron microscopy (SEM) and X-ray diffraction (XRD) are applied to investigate the microstructure and phase composition of APS WC–Co coatings before and after SPS treatment. Rietveld refinement is utilized to quantitatively determine the coatings' phase composition. Results showed that SPS treatment with the graphite punch directly in contact with the coating surface could restore the WC phase in the coating to approximately 52.3 wt.% of the overall phases in the coating, which is close to the amount of WC found in the original WC–Co feedstock used in APS coating. Comparatively, the other sample configurations employing the packing of WC–Co or YSZ powders yielded a maximum of 17.6 wt.% WC. It is believed that the direct carbon diffusion from the graphite punch during SPS played a significant role in the enhanced WC content in the coating. A comparison with the effect brought about by conventional inert atmospheric heat treatment was made by the Rietveld-refining of the XRD data from available literature, and it showed that the conventional inert atmospheric heat treatment could only cause the recrystalization of the Co_3W_3C phase and the transformation of W_2C into Co_3W_3C phase. The present study showed that the SPS working as the post-spray process, which has promising effect on reverting W_2C or other related metastable phases to the original WC in APS WC–Co coatings. Furthermore, the microhardness of the WC coating improved significantly after the SPS post-spray heat treatment.
© 2003 Elsevier B.V. All rights reserved.

Keywords: Spark plasma sintering; Plasma spray; WC; Decarburization; Rietveld refinement

1. Introduction

Tungsten carbides are used extensively throughout industry for high wear, abrasive applications as a result of their extreme hardness. There are three binary phases in the tungsten–carbon phase diagrams, namely: β-W_2C, γ-WC_{1-x} and δ-WC [1]. The γ-WC_{1-x} is thermal dynamically stable above 2535 °C, and can only be obtained at room temperature by extremely rapid cooling, e.g. in plasma sprayed layers. The β-W_2C is stable above 1250 °C and δ-WC is the only tungsten carbide phase that is stable at room temperature. The microhardness (kg/mm²) of WC is 2400 while that of W_2C is near 3000 [2]. Despite the superior hardness of W_2C, WC is typically preferred because it is less brittle than W_2C. Therefore, most commercially available tungsten carbide powders are generally composed of WC. Apart from the high hardness, WC has other unique properties such as high melting point, high wear resistance, good thermal shock resistance, thermal conductivity and good oxidation resistance [3]. WC with ductile metals such as cobalt as a binding medium that aids the cementing together of the fine WC particles is used either in bulk

*Corresponding author. Tel.: +65-6-790-5526; fax: +65-6-791-1859.

E-mail address: mkakhor@ntu.edu.sg (K.A. Khor).

sintered forms, e.g. cutting tools and dies or as surface coatings deposited by thermal spray techniques such as plasma spraying or high velocity oxy-fuel (HVOF) spray. Here, cobalt is introduced to improve their toughness so that brittle fracture among the ceramic phases can be avoided.

WC–Co coatings are widely used as protective barriers owing to their high hardness and wear-resistant characteristics. Plasma spraying in air is an easy and economical way to prepare such coatings [4–6]. More recently, high velocity oxy-fuel (HVOF) spraying was applied to deposit WC–Co coatings on metal substrate [7–9]. Due to the complex interaction among constituent elements and the reaction with the oxygen in air during the thermal spraying process, thermal sprayed WC–Co coatings exhibit complex, and multi-phase microstructures [10–14]. Phases such as WC, W_2C, W, Co amorphous/nanocrystalline binder phase and $W_2(C, O)$ or Co_3W_3C are present in the coating. In all types of reactions, the decarburization of WC is one of the main factors that reduce the hardness and wear resistance of the coatings. Recent investigations suggest that the decarburization process is as follows [11,14]. The WC will dissolve into the liquid Co phase at high temperature during spraying. Subsequently, carbon will be removed from the melt either by reaction with oxygen at the melt/gas interface or through oxygen diffusion into the rim of the molten particle, leading to CO formation. During the rapid solidification process, W_2C, W and Co(W, C) nanocrystalline/amorphous phase will form.

As the decarburization of WC strongly affects the properties of WC coatings, post-spray treatment should be employed to mitigate the effect of decarburization. Stewart et al. [12] studied the influence of conventional inert gas atmosphere heat treatment on the abrasive wear behavior of HVOF sprayed WC–Co coatings. They found that heat treatment above 600 °C results in significant phase changes within the coatings, especially the recrystallisation of the amorphous phase into one of the eta carbides (M_6C or $M_{12}C$). Heat treatment can also alter the residual stress state of the WC coating from tensile to compressive, due to the mismatch of coefficient of thermal expansion between the coating and substrate. Also, the wear behavior was improved after heat treatment. Yet, heat treatment in inert gas cannot restore the WC phase in the coating, and the recrystallized eta carbide is still more brittle than WC. Therefore, in order to further improve the properties of WC coatings, a new post-spray treatment should be applied to restore the WC phase of the coating. Spark plasma sintering (SPS) was selected as a suitable approach for such processing in this study.

SPS is a relatively new sintering technique [15–28]. In comparison to conventional sintering, SPS features the capability of sintering metal and ceramic powders quickly to full density at a fairly low temperature. Typically, the heating rate in SPS is 100–200 K/min.
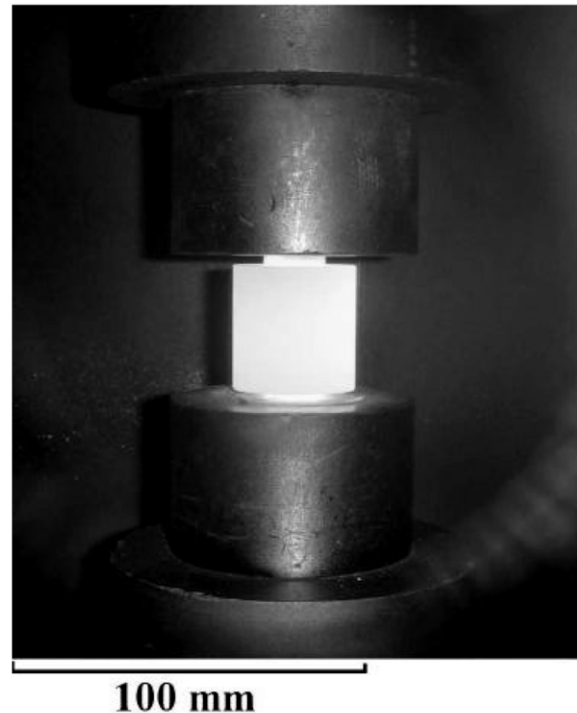

Fig. 1. Heated-up die set during SPS process.

The basic configuration of the SPS system can be found elsewhere [15–28]. Fig. 1 shows the heated-up die set in a SPS process. In the SPS system, a graphite die set is filled with the raw material powders, and is placed between the lower and upper electrodes. An external power source provides pulsed discharge to activate the surface of the contacting particles. The upper and lower electrodes apply pressure to the punches at the same time. Through charging and discharging the spaces between powder particles with electrical energy, high temperature spark discharge/plasma is effectively generated momentarily. The SPS features a very high thermal efficiency because of the direct heating of the sintering graphite mold and stacked powder materials by the large spark pulse current. SPS can readily consolidate a homogeneous, high-quality compact owing to the uniform heating, surface purification and activation made by dispersing the spark points. Due to its unique features, SPS can also be used as an effective post-spray heat treatment method for plasma sprayed coatings [29–31]. As the SPS set-up provides a reducing atmosphere, which can provide the carbon atoms needed by the restoration of WC phase in the plasma sprayed WC–Co coating, and the plasma generated in the SPS process can activate the C atoms and help the reaction-diffusion of C into the decarburized coating, the introduction of plasma can certainly enhance the carbide restoration process. There are several anticipated merits of SPS if it is introduced to the carbide restoration process. (1) The carbon-rich reduction atmosphere pro-

vides the carbon atoms. (2) The generation of spark plasma can highly activate carbon atoms. (3) The presence of the electrical field can cause high-speed diffusion of carbon due to the high-speed migration of ions. (4) The high level electric current enhances the carbon diffusion into the workpiece. (5) Rapid Joule heating can provide and maintain a homogeneous heat treatment temperature.

In this work, WC–Co coatings were prepared through atmospheric plasma spray (APS), and the SPS treatment was conducted on the coatings to reveal its effect on restoring WC within the coatings. The microstructure and phase composition were inspected with SEM and XRD. Quantitative XRD analysis was carried out using the Rietveld refinement. The effect of SPS on the WC phase recovery was discussed. The effect of SPS on the microhardness of the WC–Co coating was also investigated.

2. Experimental procedure

2.1. Plasma spraying of WC–Co coating

Commercial WC–12Co powders (Praxair, USA) were used as the raw material for plasma spray. Fig. 2a shows the particle morphologies of the powders, it can be seen that the typical WC–12Co particle has an irregular angular blocky grain shape. Stainless steel rods (SS316) (10 and 25.4 mm in diameter) were cut into 10 mm length discs, ground with 800 grit sand paper and grit blasted using SiC (-2000 μm $\sim +600$ μm) grits followed by ultrasonically cleaning for 15 min prior to plasma spraying. A computerized plasma spraying system, SG-100 (Praxair Thermal, USA) was utilized to produce the coating. All substrates were preheated before the actual spraying starts. The plasma spraying process parameters are listed in Table 1. The typical surface morphology of as-sprayed WC–Co coating is shown in Fig. 2b.

Table 1
Plasma spraying parameters

Primary gas, Ar (m³/h)	2.32
Secondary gas, He (m³/h)	1.13
Powder carrier gas, Ar (m³/h)	0.40
Net energy (kW)	14.0
Powder feed rate (g/min)	25
Water flow minimum GPM	8
Stand off distance (mm)	80 100 120

2.2. The SPS post-spray treatment

The post-spray treatment of tungsten–carbide coating was carried out using the SPS process with a temperature of 800 °C and duration of 5 min. The Sumitomo Coal Mining (SCM) SPS system Dr Sinter® Model 1050 was used for the post-spray treatment. The plasma sprayed WC coating sample is put inside a graphite die and pressed by a pair of graphite punches. Three methods were used to effect the SPS treatment of the WC coating. The first one is direct contact of WC coating with graphite die (Method A), the second method (B) involved packing the plasma sprayed coating in the original WC–Co powder, and the third method (C) is packing the coating in ZrO_2–Y_2O_3 powders. The complete preparation of the sample die is illustrated in Fig. 3. The die set was placed in the sintering chamber with the consolidation assembly being positioned between the hydraulic rams. The measurement of the die temperature is by an optical pyrometer.

The JEOL 5600 scanning electron microscope (SEM) was used to study the microstructure of the coating systems before and after SPS. X-Ray diffraction (XRD) analysis was carried out using the Philips MPD 1880 XRD equipment to determine the phases present in the coating before and after SPS treatment. Microhardness of the coatings was also measured to evaluate the effect of SPS on the mechanical property of the WC/Co coatings.
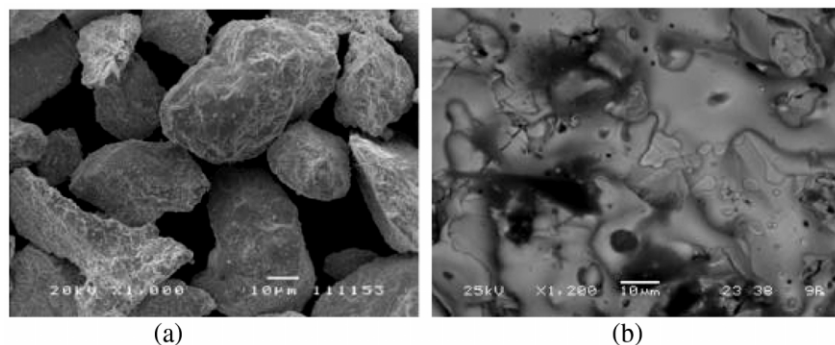

Fig. 2. SEM topographic morphology micrograph of (a) WC–Co powders and (b) As as-sprayed WC–Co coating.
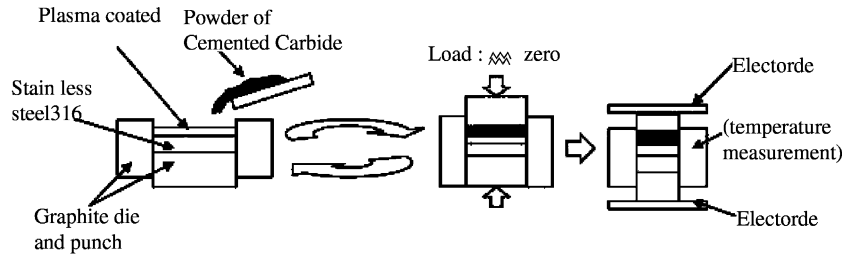
Fig. 3. Preparation of sample die set.

3. Results and discussion

3.1. SEM inspection

Fig. 4 shows the cross-sectional morphologies of as-sprayed and SPS post-treated WC–Co coatings. It can be seen that the pore density and pore size of the WC–Co coatings after SPS become smaller than that of the as-sprayed WC–Co coating, indicating coating densification occurs during SPS post-spray treatment.

3.2. X-Ray diffraction analysis

Fig. 5 shows the XRD pattern of the starting WC–Co powders with a comparison to that of the plasma sprayed WC coatings. The radiation used is Cu Kα. The raw WC–Co powder contains large amount of Co_3W_3C
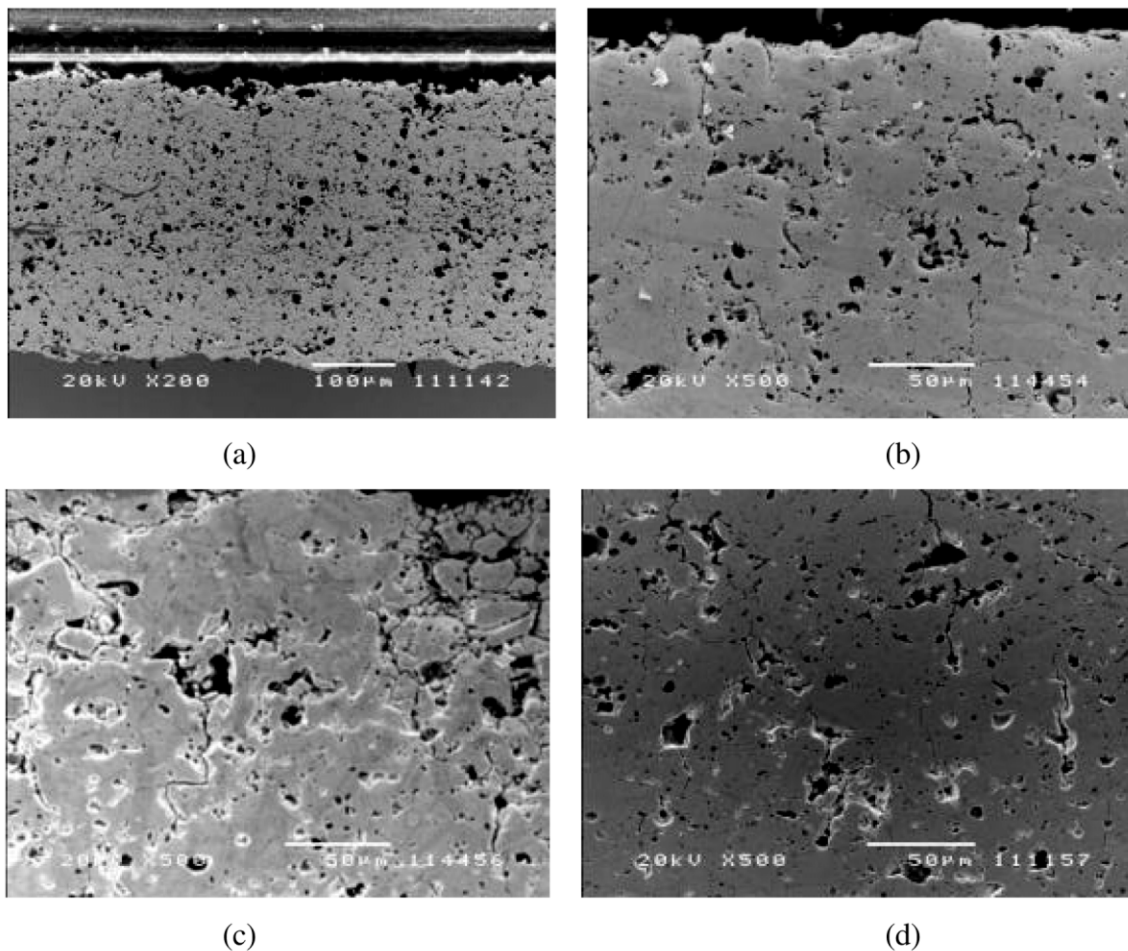

Fig. 4. SEM picture for: (a) As as-received; (b) SPS with graphite punch directly contacting with coating surface; (c) SPS with WC powder put on the top of WC coating; and (d) SPS with YSZ powder put on the top of WC coating.
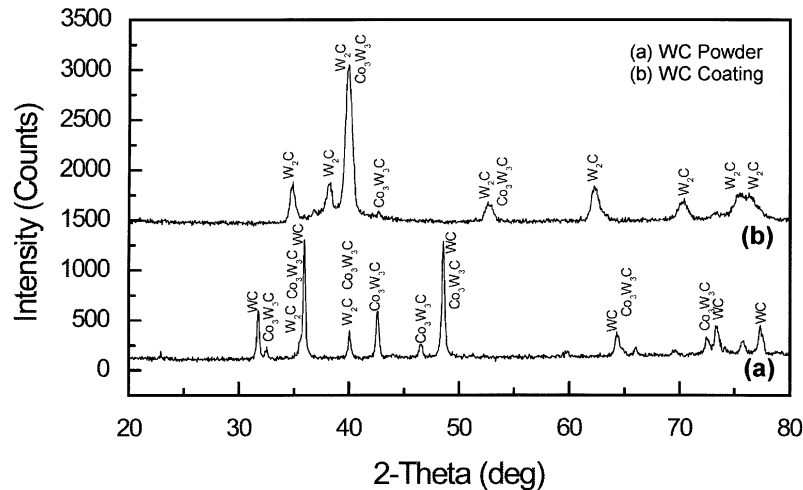
Fig. 5. XRD results for WC–Co powder and As-sprayed WC–Co coating (a) WC–Co powder (b) As-received WC–Co coating.

phase. In the XRD pattern of the as-sprayed WC–Co coating, the peaks for WC vanished, and there are evident W_2C peaks, indicating that the WC has been decarburised into W_2C under the present APS conditions.

In order to quantitatively investigate the phase composition in the WC–Co raw powders and that in the plasma sprayed coating, the Rietveld refinement was applied to obtain the phase composition. It is worth noting that in the as-received WC/Co coatings amorphous binder phase is always present due to the rapid solidification. As Rietveld refinement only take account for the crystalline phases, it is difficult to analyse the large amorphous hump in the XRD spectra. Yet, this problem can be partially settled by treating the short-range order in the amorphous phase as nanocrystal and refining the XRD spectra with associated crystals [32]. Fig. 6 shows the Rietveld refinement XRD curves of (a) WC–Co powders; and (b) as-sprayed WC coating. The quantitative contents of the phases obtained from the refinement are listed in Table 2. It is obvious that decarburization occurred during plasma spraying, resulting in a significant content of W_2C phase (approx. 60 wt.%) within the coating.

Fig. 7 shows the XRD results of WC–Co coatings after SPS treatment at 800 °C. All of the three XRD patterns corresponding to the three different SPS conditions show the peaks of WC, indicating the recovery of WC phase brought about by the SPS post-spray treatment. It shows that direct contact of the WC–Co coating with carbon punch (Method 'A') brought about the best reversion of carbon-deficient phases to WC.

The Rietveld refinement result for the three XRD patterns (Fig. 7) is shown in Fig. 8. The quantitative result is also listed in Table 2. The results confirm that the direct contact of graphite punch with WC–Co

coating surface gives the highest WC phase recovery in the coating after the SPS treatment at 800 °C, which gives an increase in WC phase composition of 52.3%. The other two SPS conditions can also induce WC phase recovery with 15.8% and 17.6%, respectively. This result highlights the principal difference in the sample packing arrangement employed in this study. In Method 'A', the restoration of WC can be attributed to concomitant C diffusion and thermal effect of the SPS treatment, while for Methods 'B' and 'C', there was only the thermal effect at work in the samples. Thus, it can be argued that the apparent diffusion of C into the plasma sprayed coating during SPS treatment when Method 'A' was employed provided a greater contribution towards the restoration of WC.

During the SPS process, a high-pulsed electrical current was applied between the upper and lower punches of the die set. Charging and discharging the spaces between the powder particles, generated spark plasma at the particle contacting point. This spark plasma can evaporate carbon atoms from the graphite punch with high activity, and deposit them on the surface of WC–Co coating, as it is believed to be the case in Method 'A'. The electrical field enhances the reaction-diffusion of carbon atoms into WC–Co coating, causing the recovery of WC phase from the W_2C phase and other carbon-deficient phases in the as-sprayed coating. It therefore, indicates that a better restoration from C-deficient phase to WC would be achieved than those areas far from coating surface. It is practically beneficial since the coating surface always plays the dominant role during its service. The restoration of WC phase on the other samples (Method 'B' and 'C') is due predominantly to thermal effect of the SPS and there would be generally, an absence of the C diffusion observed in Method 'A' since the samples have YSZ and WC–Co

as packing materials on top of the plasma sprayed coating.

In order to compare the effect of SPS treatment on the WC-restoration process, the XRD patterns of conventional inert atmosphere heat-treated WC–Co coatings [12] were also refined using the Rietveld method. The results are shown in Fig. 9. The quantitative result is listed in Table 2 as 'As-received (Stewart)' and 'Heat-treated (Stewart)'. The results show that the content of WC phase in the WC/Co coating before and after heat treatment is almost the same. This is because conventional inert atmospheric heat treatment can only result in the recrystalization of Co_3W_3C phase, and the transformation of W_2C phase into another C-deficient phase, the Co_3W_3C (η) phase, but cannot reinstate the WC

Table 2
Phase composition in the WC–Co powder and the WC coating before and after SPS

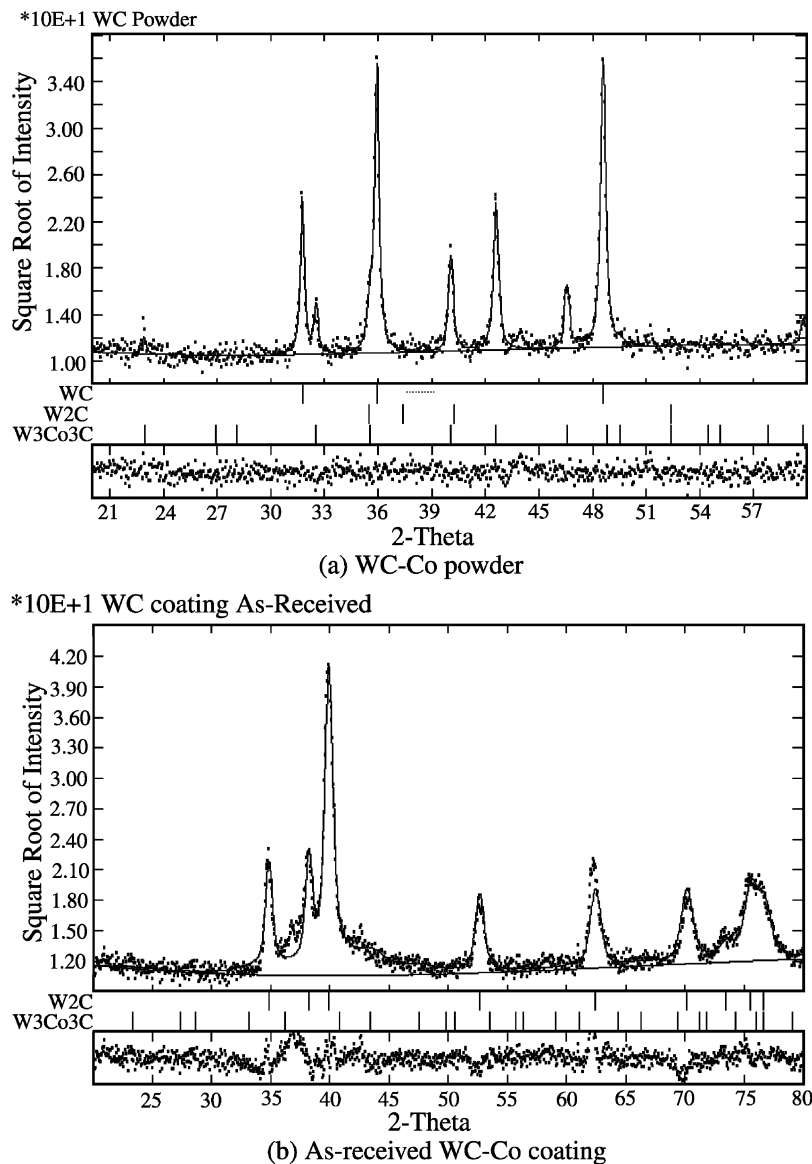| Sample	Phase		
	WC	W_2C	Co_3W_3C
(X) WC–Co powder	0.624	0.0007	0.375
(S) As-sprayed coating	0	0.600	0.400
(B) WC 800	0.158	0.380	0.462
(A) Graphite 800	0.523	0.092	0.385
(C) YSZ 800	0.176	0.381	0.443
As-received (Stewart) [11]	0.375	0.155	0.470
Heat treated (Stewart) [11]	0.360	0.008	0.631

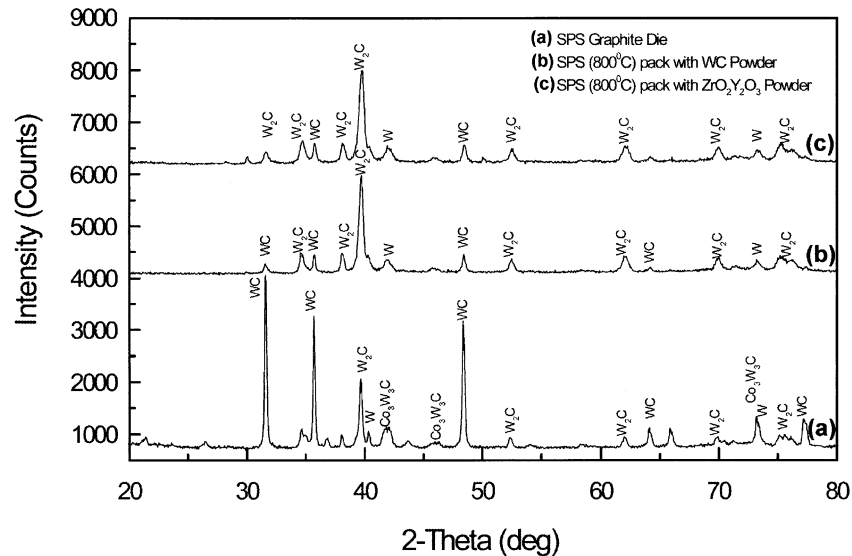Fig. 6. Rietveld refinement for WC–Co powder and as-sprayed coating.

Fig. 7. XRD pattern for WC–Co coating SPS treatment at 800 °C. (a) Rietveld refinement for WC–Co coating SPS with direct graphite punch contact with coating surface. (b) Rietveld refinement for WC–Co coating SPS with WC–Co powder put on coating surface. (c) Rietveld refinement for WC–Co coating SPS with YSZ powder put on coating surface.

phase when it is turned into C-deficient W_2C phase during the plasma spray process.

From the comparison between the Rietveld result for samples after SPS treatment and that for samples after conventional inert gas heat-treatment, one can see that there is different mechanisms involved in the diminishing/disappearance of the metastable W_2C phase in the two processes. For the conventional inert gas heat-treated WC/Co coatings, the W_2C phase is transformed into another C-deficient phase, the Co_3W_3C (η) phase. For SPS treated WC/Co coatings, because of the presents of plasma activated free carbon, the diminish of W_2C phase is followed by the diffusion-reaction of carbon with all kinds of carbon-deficient phases such as W_2C and amorphous binding phase in the coating to form the WC phase, and the WC phase is reinstated in this way.

3.3. Microhardness investigation

The microhardness values taken from the polished cross-sections of the WC–Co coatings before and after SPS post-treatment are shown in Fig. 10. A remarkable improvement of the coating hardness is demonstrated after the SPS treatment. In fact an increase of over 200% on the as-sprayed microhardness was found in the SPS samples. This is believed to be due to the dual achievements of the SPS process, namely, the densification of the coating and the recovery of the WC phase in the coating. The values recorded were found to have corresponded well with the phases observed in the XRD spectra of the SPS samples. The coating that was treated through direct contact with graphite punch (Method A)

demonstrated the highest microhardness value followed by the coating embedded in WC–Co powders (Method B) and finally, coating packed in YSZ powders (Method C).

4. Conclusions

APS WC–Co coating was heat-treated by spark plasma sintering at 800 °C with a soak time of 5 min. SEM and XRD investigation revealed the changes in the microstructure and phase compositions in the WC–Co coating before and after the SPS treatment. The XRD patterns before and after SPS was refined by the Rietveld method. The following results are concluded:

1. The post-spray SPS treatment can modify the microstructure of the plasma sprayed WC–Co coatings by aiding the restoration of the WC phase in the coating and closure of the majority of pores and crack networks in the plasma sprayed coating;
2. SPS is capable of effectively recovering the WC phase from W_2C and other ancillary phases in the WC–Co coating. Method A (direct contact of graphite punch to coating surface during the SPS treatment) was found to provide the highest WC phase recovery rate of up to 52.3%. This is attributed to the diffusion of C into the plasma sprayed coating surface and effectively enforcing the conversion of the phases therein to WC. This is reflected in Method 'A' yielding 52.3% WC as compared to 17.6% WC in Method 'C' (when YSZ was used as packing material). Other sample packing configurations in SPS such as packing with WC–Co or YSZ were found to be less effective. Nonetheless, enhancement of the
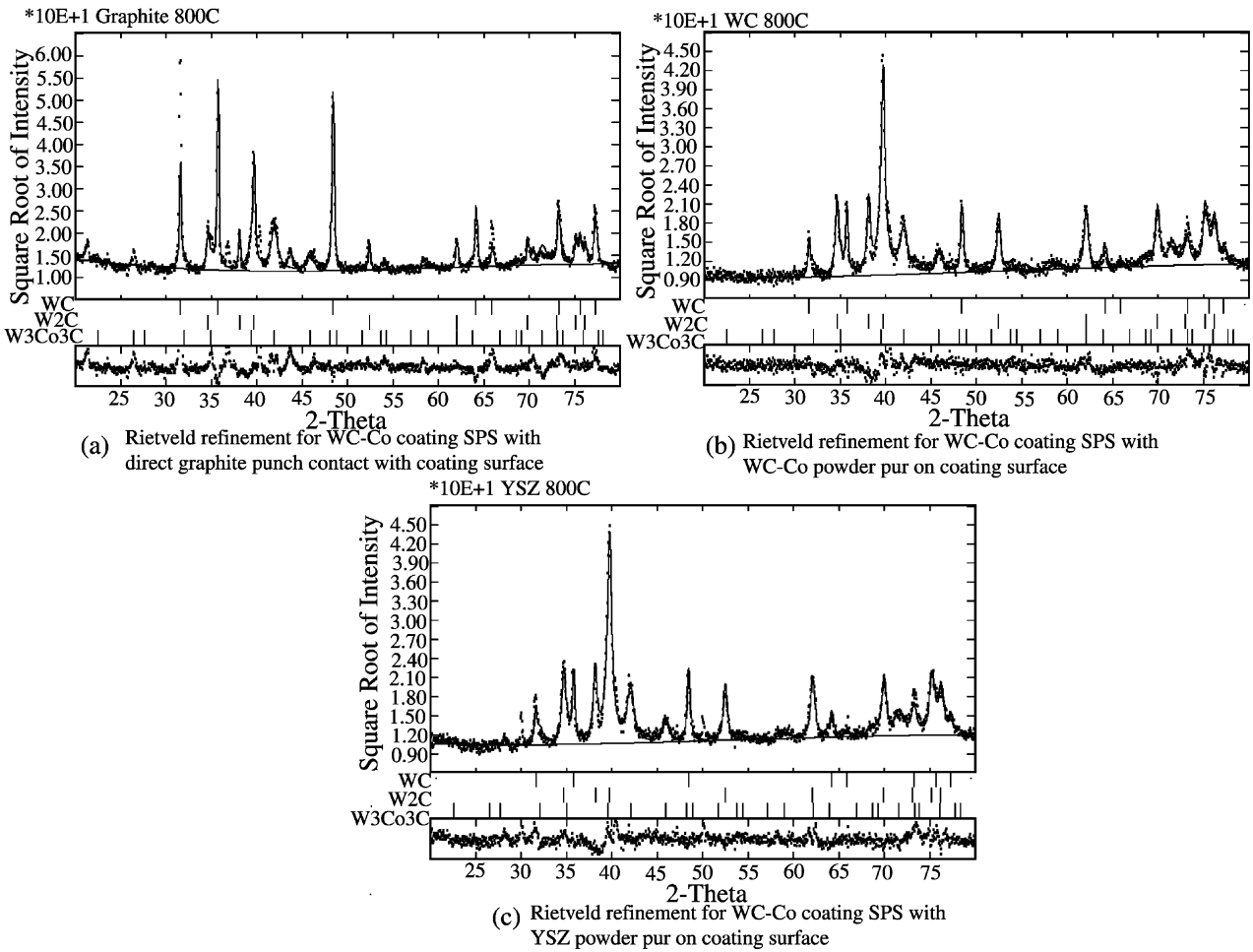
Fig. 8. Rietveld refinement for WC–Co coating after SPS post-treatment (a) As-received HVOF WC–Co coating (WC- 17wt.% Co). (b) After inert atmospheric heat treatment at 800 °C for 0.8 h, showing the recrystalization of Co_3W_3C phase and the transformation of W_2C to Co_3W_3C.
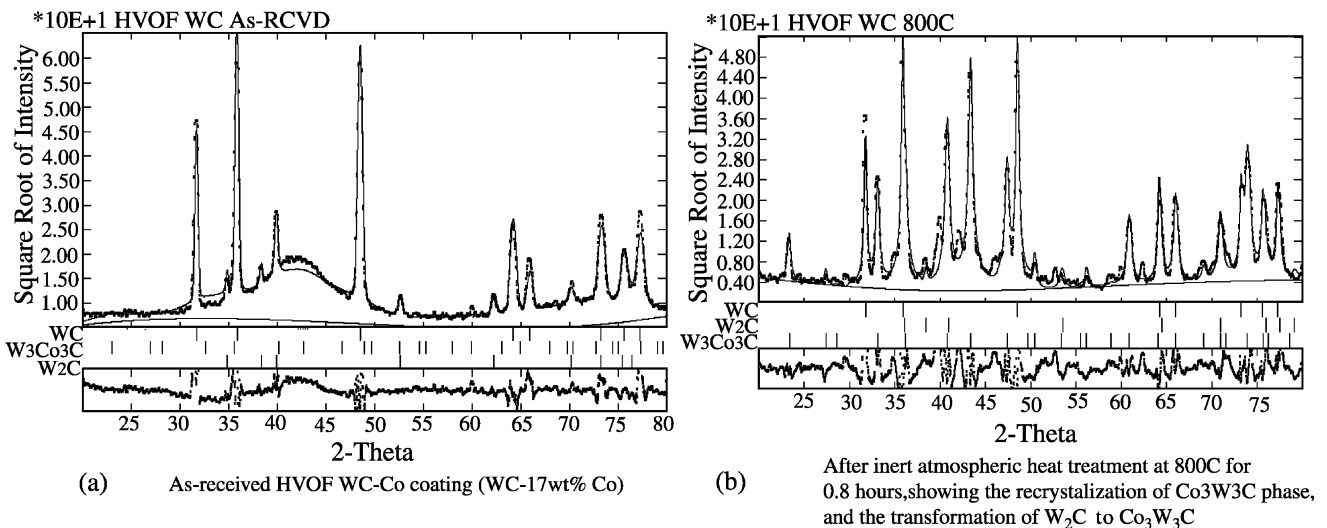

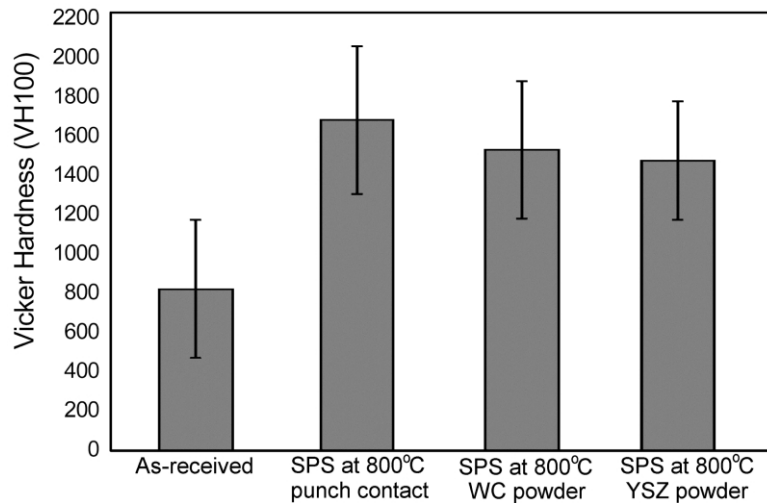Fig. 9. Rietveld refinement for the XRD results in literature [12].

Fig. 10. Microhardness of WC–Co coatings before and after SPS post spray treatment.

coatings' properties was evident, and was attributed to solely the thermal effect of the SPS treatment. It can also be seen that the C diffusion was more efficacious in the restoration of WC, where the amount of WC found is approximately three-fold of the amount found when there was an absence of C diffusion;

3. The microhardness of the WC–Co coating is increased after SPS post-spray heat treatment, indicating SPS enhances the mechanical property of the coatings. The increase in hardness values corresponded with the amount of WC in the SPS samples.

References

[1] T.B. Massalski (Ed.-in-Chief), H. Okamoto, P.R. Subramanian, L. Kacprzak (Eds.), Binary Alloy Phase Diagrams, 2nd Edn, Vol. 1. ASM International, Materials Park, Ohio, Publisher, William W. Scott, Jr. 1990, 895–896.

[2] D. Tu, S. Chang, C. Chao, C. Lin, Tungsten carbide phase transformation during the plasma spray process, J. Vac. Sci. Technol. A3 (6) (1985) 2479–2482.

[3] B. Vamsi Krishna, V.N. Misra, P.S. Mukherjee, P. Sharma, Microstructure and properties of flame sprayed tungsten carbide coatings, Int. J. Refract. Met. Hard Mater. 20 (2002) 355–374.

[4] J. Voyer, B.R. Marple, Sliding wear behavior of high velocity oxy-fuel and high power plasma spray-processed tungsten carbide-based cermet coatings, Wear 225–229 (Part 1) (April 1999) 135–145.

[5] Y. Qiao, Y. Liu, T.E. Fischer, Sliding and abrasive wear resistance of thermal-sprayed WC–Co coatings, J. Therm. Spray Technol. 10 (1) (March 2001) 118–125.

[6] Y.C. Zhu, C.X. Ding, K. Yukimura, T. Danny Xiao, P.R. Strutt, Deposition and characterization of nanostructured WC–Co coating, Ceram. Int. 27 (6) (2001) 669–674.

[7] C.-J. Li, Y.-Y. Wang, T. Wu, G.-C. Ji, A. Ohmori, Effect of types of ceramic materials in aggregated powder on the adhesive strength of high velocity oxy-fuel sprayed cermet

coatings, Surf. Coat. Technol. 145 (1–3) (1 August 2001) 113–120.

[8] D. Toma, W. Brandl, G. Marginean, Wear and corrosion behaviour of thermally sprayed cermet coatings, Surf. Coat. Technol. 138 (2/3) (16 April 2001) 149–158.

[9] H. Liao, B. Normand, C. Coddet, Influence of coating microstructure on the abrasive wear resistance of WC/Co cermet coatings, Surf. Coat. Technol. 124 (2/3) (21 February 2000) 235–242.

[10] C. Verdon, A. Karimi, J.L. Martin, Study of high velocity oxy-fuel thermally sprayed tungsten carbide based coatings, Part 1: microstructures, Mater. Sci. Eng. A246 (1998) 11–24.

[11] D.A. Stewart, P.H. Shipway, D.G. McCartney, Microstructural evolution in thermally sprayed WC–Co coatings: comparison between nanocomposite and conventional starting powders, Acta Mater. 48 (200), 1593–1604.

[12] D.A. Stewart, P.H. Shipway, D.G. McCartney, Influence of heat treatment on the abrasive wear behavior of HVOF sprayed WC–Co coatings, Surf. Coat. Technol. 105 (1998) 13–24.

[13] H. Chen, I.M. Hutchings, Abrasive wear resistance of plasma-sprayed tungsten carbide–cobalt coatings, Surf. Coat. Technol. 107 (1998) 106–114.

[14] B.H. Kear, G. Skandan, R.K. Sadangi, Factors controlling decarburization in HVOF sprayed nano-WC/Co hard-coatings, Scr. Mater. 44 (2001) 1703–1707.

[15] D.L. Johnson, Microwave and plasma sintering of ceramics, Ceram. Int. 17 (1991) 295–300.

[16] S.H. Risbud, C.H. Shan, Fast consolidation of ceramic powders, Mater. Sci. Eng. A 204 (1995) 146–151.

[17] H. Su, D.L. Johnson, Sintering of alumina in microwave-induced oxygen plasma, J. Am. Ceram. Soc. 79 (1996) 3199–3201.

[18] J. Hong, L. Gao, S.D.D.L. Torre, H. Miyamoto, K. Miyamoto, Spark plasma sintering and mechanical properties of ZrO_2 (Y_2O_3)–Al_2O_3 composites, Mater. Lett. 43 (2000) 27–31.

[19] C.H. Shan, S.H. Risbud, Rapid consolidation of Bi–Pb–Ca–Cu–O powders by a plasma activated sintering process, Mater. Sci. Eng. B 26 (1994) 55–60.

[20] L. Gao, H.Z. Wang, J.S. Hong, H. Miyamoto, K. Miyamoto, Y. Nishikawa, et al., SiC–ZrO_2(3Y)–Al_2O_3 nanocomposites superfast densified by spark plasma sintering, Nanostructured Mater. 11 (1999) 43–49.

[21] J.R. Groza, A. Zavaliangos, Sintering activation by external electrical field, Mater. Sci. Eng. A 287 (2000) 171–177.

[22] M. Omori, Sintering, consolidation, reaction and crystal growth by spark plasma system (SPS), Mater. Sci. Eng. A 287 (2000) 183–188.

[23] J.R. Groza, S.H. Risbud, K. Yamazaki, Plasma activated sintering of additive-free AlN powders to near-theoretical density in 5 min, J. Mater. Res. 7 (1992) 2643–2645.

[24] S.H. Risbud, J.R. Groza, M.J. Kim, Clean grain boundaries in aluminum nitride ceramics densified without additives by a plasma-activated sintering process, Phil. Mag. B 69 (1994) 525–533.

[25] J.E. Hensley Jr, S.H. Risbud, J.R. Groza, K. Yamazaki, Plasma-activated sintering of aluminum nitride, J. Mater. Eng. Perform. 2 (1993) 665–670.

[26] K. Yamazaki, S.H. Risbud, H. Aoyama, K. Shoda, PAS (plasma activated sintering): transient sintering process control for rapid consolidation of powders, J. Mater. Proc. Technol. 56 (1996) 955–965.

[27] M. Tokita, Development of large-size ceramic/metal bulk FGM fabricated by spark plasma sintering, Materials Science Forum, Proceedings of the 1998 5th International Symposium on Functionally Graded Materials, FGM 1998, October 26–29 1998, Dresden, Germany, 1999, Vol. 308–311, pp. 83–88.

[28] N. Kuramoto, H. Taniguchi, I. Aso, Sintering and properties of high purity AlN ceramics, in: M.F. Fan, K. Niwa, H.M. O'Bryan, W.S. Young (Eds.), Ceramic Substrates and Packages for Electronic Applications. Advances in Ceramics, 26, American Ceramic Society Inc, Westerville, Ohio, 1989, pp. 107–119.

[29] B. Prawara, H. Yara, Y. Miyagi, T. Fukushima, Spark plasma sintering as a post-spray treatment for thermally-sprayed coatings, Surf. Coat. Technol. 162 (2003) 234–241.

[30] L.G. Yu, K.A. Khor, H. Li, P. Cheang, Effect of spark plasma sintering on the microstructure and in vitro behavior of plasma sprayed HA coatings, Biomaterials 24 (2003) 2695–2705.

[31] K.A. Khor, L.G. Yu, O. Andeerson, G. Stephani, Effect of spark plasma sintering (SPS) on the microstructure and mechanical properties of randomly packed hollow sphere (RHS) cell wall. Mater. Sci. Eng. A (In Press).

[32] M.R. Ebeid, S.K. Abdelraheem, E.M. Abdel-Minem, K. Abdel-Hady, A.A. Ramadan, Verification of crystallite theory of glass. Modeling using rietveld method, Egypt J. Sol. 23 (1) (2000) 1–11.